Thermally Induced Formation of HF_4TCNQ^- in F_4TCNQ-Doped Regioregular P3HT

Kristen E. Watts,[a] Bharati Neelamraju,[b] Maximilian Moser,[c] Iain McCulloch,[c,d] Erin L. Ratcliff,[b*] and Jeanne E. Pemberton[a*]

[a] Department of Chemistry and Biochemistry
[b] Department of Materials Science and Engineering
University of Arizona, Tucson, AZ, USA

[c] Department of Chemistry and Centre for Plastic Electronics
Imperial College London
London, UK

[d] KSC, King Abdullah University of Science and Technology
Thuwal, Saudi Arabia

Abstract

The prototypical system for understanding doping in solution-processed organic electronics has been poly(3-hexylthiophene) (P3HT) p-doped with 2,3,5,6-tetrafluoro-7,7,8,8-tetracyanoquinodimethane (F_4TCNQ). Multiple charge transfer states, defined by the fraction of electron transfer to F_4TCNQ, are known to coexist and are dependent on polymer molecular weight, crystallinity, and processing. Less well understood is the loss of conductivity after thermal annealing of these materials. Specifically, in thermoelectrics, F_4TCNQ-doped regioregular (rr) P3HT exhibits significant conductivity losses at temperatures lower than other thiophene-based polymers. Through detailed spectroscopic investigation of progressively heated P3HT films co-processed with F_4TCNQ, we demonstrate that this diminished conductivity is due to formation of the non-chromophoric, weak dopant HF_4TCNQ^-. This species is likely formed through hydrogen abstraction from the alpha aliphatic carbon of the hexyl chain at the 3-position of thiophene rings of rr-P3HT. This reaction is eliminated for polymers with ethylene glycol-containing side chains, which retain conductivity at higher operating temperatures. In total, these results provide a critical materials design guideline for organic electronics.

KEYWORDS

Organic Electronics, Doped Semiconducting Polymers, F_4TCNQ-doped P3HT, Ethylene Glycol-functionalized Semiconductors, Design Guidelines

*Corresponding authors: pembertn@email.arizona.edu, ratcliff@email.arizona.edu

TOC Graphic

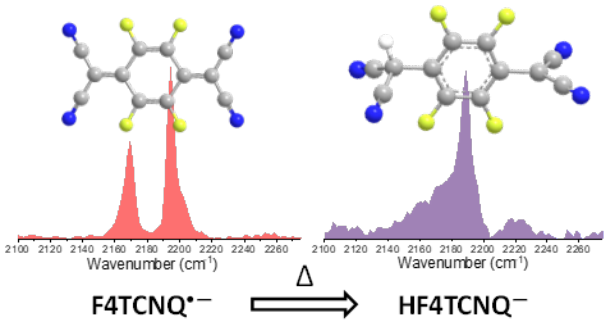
2100 2120 2140 2160 2180 2200 2220 2240 2260
Wavenumber (cm-1)
2100 2120 2140 2160 2180 2200 2220 2240 2260
Wavenumber (cm-1)
Δ
F4TCNQ•−
HF4TCNQ−

Molecularly-doped organic semiconductors are of interest for use in organic electronic devices including thermoelectrics,[1-4] light emitting diodes,[5] photovoltaics,[6-10] and field effect transistors.[11-15] Although organic electronics are experiencing an increased presence in the market, critical challenges remain for long-term use of these materials, including low conductivity and chemical stability. Increased conductivity is typically achieved by doping with p- or n-type species that generate mobile free charge carriers from intermolecular electron transfer reactions between the matrix and dopant.[16] External operational factors such as light exposure and heat can accelerate chemical instability of active layers and negatively impact functional lifetime. This instability can be manifested in multiple ways, including undesired side reactions leading to the formation of degradation products and/or morphological changes in matrix microstructure. This work focuses on understanding thermal stability in the model system of 2,3,5,6-tetrafluoro-7,7,8,8-tetracyanoquinodimethane (F_4TCNQ)-doped regioregular poly(3-hexylthiophene) (rr-P3HT) and the implications of this thermal stability for conductivity of the active layer.

Early reports on this well-studied system focused on the elucidation of key structure-property relationships. Doping efficiency (as indicated by conductivity) was shown to be dependent on dopant concentration in co-processed films and was attributed to the presence of dopants only in amorphous domains of rr-P3HT at low concentrations with intercalation into crystalline domains at higher concentrations.[17] It was later found that use of a sequential processing method provides improved doping efficiency due to better doping predictability and the ability to direct the dopant to crystalline or amorphous regions of the polymer by choice of solvent and post-doping film processing.[16] Méndez et al. provided an energy description of the doping process that identified two possible doping pathways: integer charge transfer (ICT) resulting from full electron donation from the rr-P3HT to F_4TCNQ, or formation of a partial charge transfer complex (CPX)

due to hybridization of dopant and host molecular orbitals.[18-19] The co-existence of these two charge transfer states in F_4TCNQ-doped rr- and regiorandom (rra)-P3HT thin films has recently been reported from these laboratories, with the relative amounts of each being generally correlated with P3HT matrix microstructure.[20]

Despite significant advancements in understanding this system, chemical and thermal stability of the relevant doped states necessary for longevity in functional properties have generally been overlooked in prior studies. We have shown that although the ICT state appears to be kinetically favored, the more thermodynamically stable of these states is the CPX state in co-processed films, serving as charge trap sites that reduce conductivity.[21] However, there is a dearth of information about the relative thermal stability of these two states. Past work has suggested the contributions of three possible factors to explain the thermal instability of small molecule doped polymer active layers: 1) chemical reaction of molecules in the active layer upon exposure to thermal stress;[22] 2) change in or disappearance of charge transfer states;[21, 23] and 3) the physical loss and/or migration of dopant.[16, 24-26] All three processes have important implications for efficiency of the active layer, and one or more of these processes may be inter-related.

The stability of pure rr-P3HT to thermal stress has been well characterized,[22] but recent efforts to characterize the stability of F_4TCNQ in F_4TCNQ-doped polymer blends have resulted in contradictory results, particularly at moderate temperatures between 80 and 120 °C.[24-25, 27] Thermal stability studies of F_4TCNQ in rr-P3HT,[25] s-P3MEET[25] and p($g_4$2T-T)[24] have been reported, with F_4TCNQ-doped rr-P3HT exhibiting significantly poorer thermally stability than the other two systems. Based on the lower electrical conductivity of F_4TCNQ-doped rr-P3HT films relative to F_4TCNQ-doped s-P3MEET and p($g_4$2T-T) films after thermal treatment, this instability has been

proposed to result from differences in F_4TCNQ dopant sublimation from the three matrices.[24-25] However, no direct probe of F_4TCNQ presence was utilized in this prior work.

The starting hypothesis for the work reported here is that the chemical stability of the dopant, existing primarily as a radical anion,[20] plays a critical role in the thermally-induced degradation phenomena observed in F_4TCNQ-doped rr-P3HT films at moderate temperatures. Thus, this work was undertaken with the goal of defining with greater chemical specificity the thermal instability of F_4TCNQ within doped rr-P3HT films at moderate temperatures (<120 °C) and correlating this behavior with the overall electrical conductivity of the film.

Figure 1 summarizes the changes in optoelectronic properties and corresponding conductivity measured on co-processed thin (~15 nm) films of this system, as well as elemental quantification of possible F_4TCNQ loss using x-ray photoelectron spectroscopy (XPS). Briefly, UV-vis spectroscopy and conductivity measurements were performed on P3HT films with F_4TCNQ dopant mole fraction (χ_{F4TCNQ}) of 0.096 (defined by solution composition of F_4TCNQ and thiophene equivalents prior to spin-casting) as they were progressively heated in a glove box from room temperature to 60, 80, 100, and 120 °C, being held at each temperature for 5 min. Immediately after film casting, the UV-Vis spectrum (Figure 1a) clearly indicates a doped largely crystalline rr-P3HT film (black) by the presence of the strong π - π^* P3HT band at ~2.5 eV and a broad polaron band from 1.8 to 1.4 eV. The ICT $F_4TCNQ^{\bullet-}$ spectral signatures are still distinct at ~1.6 and ~1.4 eV, with a shoulder just below 3.0 eV.[24-25] As the sample is progressively heated, loss of the $F_4TCNQ^{\bullet-}$ absorption signatures is observed, with a fraction of the P3HT polaronic absorbance remaining even at 120°C. Two contributions to this loss can be postulated: loss of $F_4TCNQ^{\bullet-}$, possibly with reformation of neutral F_4TCNQ, or changes in P3HT microstructure leading to reorientation of $F_4TCNQ^{\bullet-}$. For randomly oriented P3HT films, changes in orientation

of $F_4TCNQ^{\bullet-}$ may make minor contributions to the decrease in intensity of the 1.4 eV UV-vis band.[28] However, given that our UV-vis spectroscopy utilized an unpolarized source, these contributions are expected to be minimal to insignificant. Loss of $F_4TCNQ^{\bullet-}$ is much more likely. However, there is no evidence for conversion to neutral F_4TCNQ, which would result in a new band at 3.2 eV.[24]

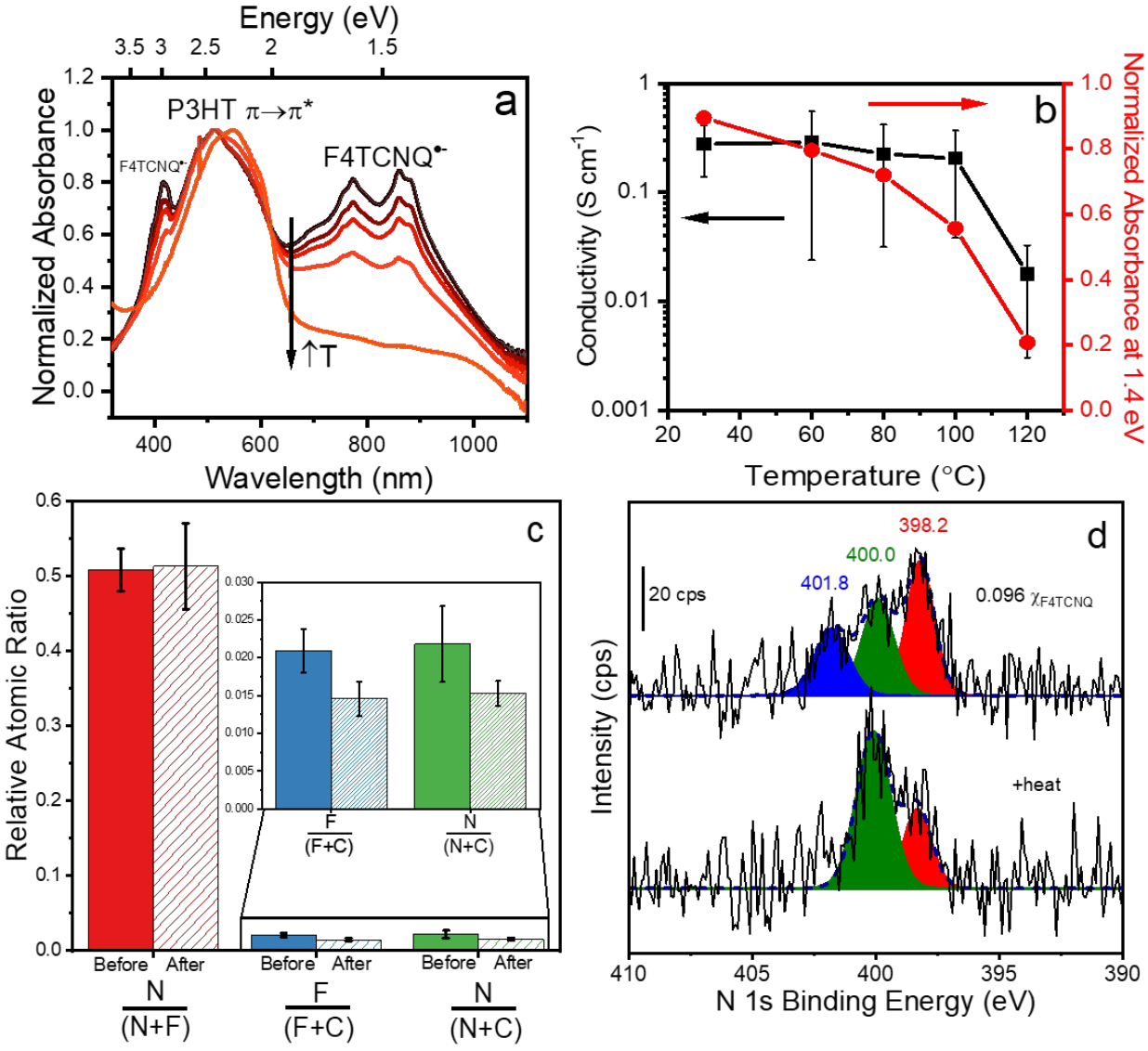

Figure 1. (a) UV-Vis absorption spectra from a 15 nm-thick film of 0.096 χ_{F4TCNQ} doped rr-P3HT progressively heated in a glove box for 5 min each at 60, 80, 100 and 120°C. (b) Conductivity from 3 to 5 devices (left axis) and change in normalized $F_4TCNQ^{\bullet-}$ absorption at 1.4 eV (right axis) with annealing temperature. (c) Relative atom ratios for N/(N+F), F/(F+C), and N/(N+C) before (solid) and after (hashed) heating. (d) N 1s XPS spectra from 0.096 χ_{F4TCNQ} film at room temperature (top) and after (bottom) progressive sequence of heating described in (a).

Loss of the 1.4 eV band from $F_4TCNQ^{\bullet-}$ is quantified in Figure 1b (right axis), which rationalizes, at least in part, the loss in conductivity also shown in Figure 1b.[17] In Figure 1b, the conductivity for the same progressive heating sequence decreases from 2.8 x 10^{-1} to ~1.8 x 10^{-2} S cm^{-1}. Temperature-dependent decreases in conductivity of F_4TCNQ-doped P3HT have been reported previously and attributed to sublimation of F_4TCNQ.[16, 24-27, 29] However, the conductivity of an undoped rr-P3HT film with an analogous heat treatment is ~10^5 times lower (5 x 10^{-7} S cm^{-1}) than that of the thermally annealed doped P3HT film, indicating retention of at least some of the doped film in a conductive state after heating. If it is assumed that the conductivity loss of the doped film is due only to a loss of dopant, with minimal change to charge mobility, then one can use the previously reported conductivity increment per unit dopant to estimate the fractional dopant loss represented by the observed conductivity decrease. Specifically, Duong et al. reported a conductivity increase of 13.3 S cm^{-1} per unit mole fraction F_4TCNQ dopant added for χ_{F4TCNQ} between 0.031 and 0.17.[17] Using this value, the decrease in conductivity observed here would suggest an equivalent loss of 20-45% in dopant mole fraction after heating if dopant loss were the mechanism responsible for the conductivity decrease. This large of a F_4TCNQ dopant loss would be readily observable by XPS if loss occurred.

Figure 1c shows XPS results in terms of relative atom ratios for different elements before and after heat treatment. These results indicate no statistically significant change after heating for N/(N+F) (both elements unique to F_4TCNQ) in the near-surface region of these films, consistent with minimal thermal decomposition or thermally-driven loss of dopant. Similarly, the relative atom ratios F/(F+C) and N/(N+C) are all within the standard deviations of multiple independent experiments on films before and after thermal annealing indicating conclusively that, for this thermal treatment, F_4TCNQ does not sublime as has been previously reported.[16, 24-27, 29] We note

that the F/(F + C) ratio for this film is slightly larger than the expected value of 0.015 in the pristine film before heating, but then becomes equal to the expected value after heating. This suggests slight segregation of F_4TCNQ to the upper portions of the pristine doped film before heating with homogenization of the film induced by heating while losing none of the F_4TCNQ to sublimation.

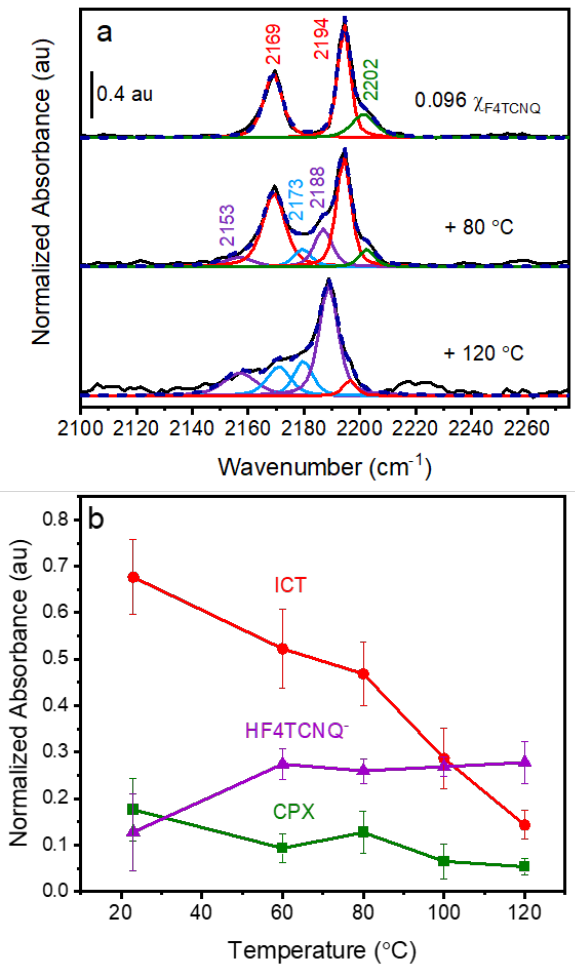

Figure 2. (a) FTIR spectral fits at three temperature points during the progressive heating of a 15 nm-thick film of 0.096 χ_{F4TCNQ} in rr-P3HT. The red fit line corresponds to the ICT state of F_4TCNQ, the green line to the CPX state of F_4TCNQ, and the purple line to HF_4TCNQ^-. Cyan peaks were added for a better fit but are currently unidentified. (b) Changes in ICT (2194 cm^{-1}, red), CPX (2202 cm^{-1}, green), and HF_4TCNQ^- (2188 cm^{-1}, purple) absorbance values normalized to the $\nu(CH_2)_{ip}$ at 2852 cm^{-1} for progressively heated 0.096 χ_{F4TCNQ} films.

Thermal annealing does elicit spectral changes in the N 1s core level spectra (Figure 1d) in terms of the binding energies and relative intensities of peaks observed. However, definitive assignment of these peaks requires a better understanding of the molecular level changes induced in the films by the thermal annealing process. Thus, FTIR spectroscopy was used to provide additional chemical insight.

FTIR spectroscopy can aid in clarifying the specific molecular nature of dopant forms in the film, as frequency shifts of the ν(C≡N) mode are highly sensitive to the chemical state of the F_4TCNQ, including the degree of charge transfer between F_4TCNQ and the P3HT.[19, 23, 30-33] The FTIR spectra in Figure 2a

(unnormalized spectra in Figure S1) show little evidence for CPX in the films after final heating. A low absorbance broad band at higher frequency may indicate a small contribution from neutral F_4TCNQ. However, most notable after heating is the appearance of two new bands in the ν(C≡N) region at 2188 and 2153 cm^{-1} at frequencies between known bands of the ICT state ($F_4TCNQ^{\bullet-}$, ν = 2194 cm^{-1}) and the dianion (F_4TCNQ^{2-}, ν = 2164 cm^{-1}).[31, 34-35] These two bands increase in intensity with annealing temperature, dominating the IR spectrum in films heated to 120 °C (Figure 2a). Exposure to long-wavelength UV light has no impact on this chemistry as reflected in the FTIR spectra (see Figure S2). Significantly, retention of the overall ν(C≡N) envelope amplitude with heating for all dopant concentrations (see Figure S1) further corroborates the assertion that a significant amount of F_4TCNQ does not sublime.

The correlation between frequency and F_4TCNQ charge state allows assignment of the two new bands in the ν(C≡N) region that appear with heating. The frequencies of these bands suggest F_4TCNQ species with electron density between that of the anion (ICT) and the dianion. Le et al. investigated the basicity of the reduced states of F_4TCNQ in acetonitrile solutions containing trifluoroacetic acid (TFA) via electrochemistry and UV-vis spectroelectrochemistry,[36-37] wherein they demonstrated a strong propensity for rapid proton transfer from TFA to F_4TCNQ^{2-} to yield HF_4TCNQ^- (K_{eq} = 3 x 10^3; k_f = 1 x 10^{10} M^{-1} s^{-1}).[36] Further, they noted that HF_4TCNQ^- has a low molar absorptivity in the UV-vis region resulting in loss of the dianion band without growth of any new electronic bands. In contrast, in similar FTIR spectroelectrochemical experiments on F_4TCNQ in acetonitrile solutions containing acids recently reported from this laboratory,[38] new bands in the ν(C≡N) region of the FTIR spectra at 2183 and 2153 cm^{-1} were observed that match in frequency the two new bands observed in the heated F_4TCNQ-doped rr-P3HT films studied here. In the solution FTIR spectroelectrochemistry study, the 2183 and 2153 cm^{-1} bands were

assigned to the ν(C-C≡N) symmetric stretching modes from HF_4TCNQ^- for the unprotonated and protonated sides, respectively (as confirmed by spectral simulations, see Figure S3), that forms by a concerted proton-coupled electron transfer.[38]

Further evidence for the presence of HF_4TCNQ^- in the heated films studied here comes from examination of the ν(C=C) region of the FTIR spectrum between 1450 and 1600 cm^{-1} (Figure S4). New bands at 1485, 1505, and 1630 cm^{-1} correspond to similar solution-state bands from HF_4TCNQ^- observed in our previous study.[38] Thus, we confidently conclude that loss of the ICT state with heating, previously attributed to F_4TCNQ sublimation, is instead due to the formation of HF_4TCNQ^- within these films. This explanation rationalizes loss of the ICT UV-vis signal but with retention of a significant conductivity relative to undoped rr-P3HT after heating. HF_4TCNQ^- is clearly non-chromophoric in the UV-vis region and serves as a weaker dopant of P3HT than $F_4TCNQ^{\bullet-}$.

Now that the various molecular forms of the F_4TCNQ dopant in these films are identified, we can return to the N 1s XPS data of Figure 1d. Prior to heating, three N 1s peaks are observed in the pristine film. These have been commonly assigned to the ICT species (binding energy 398.2 eV), the neutral F_4TCNQ state (400.0 eV),[39-41] and a shake-up peak associated with the ICT species (401.8 eV). Similar peaks at 398.6 and 400.2 eV were reported for $TCNQ^{\bullet-}$,[40-41] and similar fits including a shake-up peak have also been reported for F_4TCNQ.[41-42] With thermal annealing, a significant loss of the 398.2 and 401.8 eV peaks is observed with concomitant loss of the ICT bands in the UV-vis spectrum (Figures 1a) and the ICT ν(C≡N) band in the FTIR spectrum, thus confirming the assignment of these peaks to the ICT state of F_4TCNQ. Interestingly, however, the N 1s peak at 400.0 eV is retained to a much greater extent after heating and is therefore assigned to HF_4TCNQ^-. This peak must either have a coincidental overlap in binding energy with that of

neutral F_4TCNQ or some small amount of HF_4TCNQ^- must be in the films examined by XPS before heating, possibly as the result of handling and transport to the surface analysis laboratory. DFT calculations of the charge distribution on F_4TCNQ and HF_4TCNQ^- (see Figure S5) corroborate the coincidental overlap in binding energy by the similarity of the calculated Mulliken charges of the nitrogen in F_4TCNQ (-0.51) and the nitrogen on the protonated side of HF_4TCNQ (-0.48). The absence of a shake-up peak for HF_4TCNQ^- is unremarkable, since the intensity of a shake-up process is related to the square of the overlap integral between the valence electron wave functions of the initial and final states of the system.[40] The electronic structure of HF_4TCNQ^- is expected to be substantially different from that of F_4TCNQ or $F_4TCNQ^{\bullet-}$, consistent with its non-existent absorption in the UV-vis spectrum. Thus, in total, the UV-Vis, FTIR and XPS spectral data collectively indicate a growth of HF_4TCNQ^- at the expense of $F_4TCNQ^{\bullet-}$ upon thermal annealing. We note that this formation of HF_4TCNQ^- in turn introduces a slight change in polymer microstructure, as indicated by the in- and out-of-plane grazing incidence wide angle x-ray scattering measurements in Figure S6, although the edge-on orientation of the structure is retained (Figure S7).

We next focus on the possible mechanisms for HF_4TCNQ^- formation in the solid state. In solution, HF_4TCNQ^- can be formed even in the presence of weak proton donors.[38] We hypothesize that rr-P3HT, more specifically a hydrogen on the alpha-carbon of the hexyl chains, serves as the hydrogen source based on the well-known reactivity of this site and the fact that these heating experiments were conducted under inert conditions.[22, 43-44] Two possible mechanisms are proposed for formation of HF_4TCNQ^- in Scheme 1. The first mechanism involves hydrogen abstraction by $F_4TCNQ^{\bullet-}$ from the aliphatic carbon atom alpha to the 3-position of the quinoidal thiophene ring to form HF_4TCNQ^-, followed by rapid recombination of the radicals on the rr-P3HT backbone

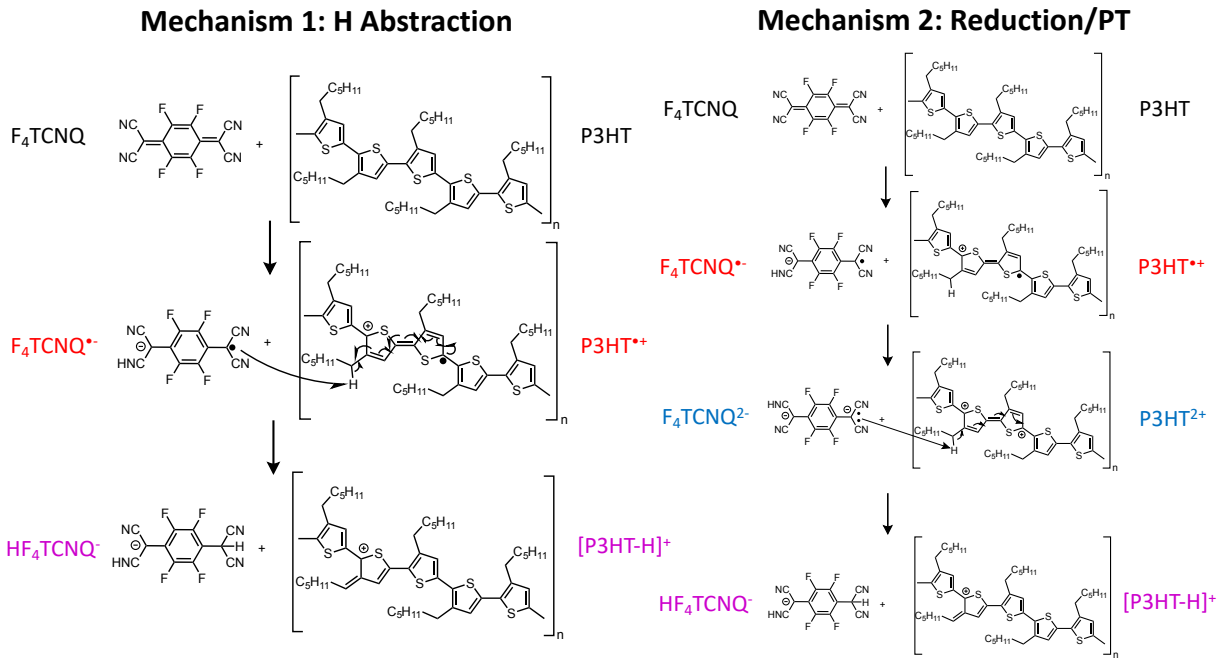

Scheme 1. Proposed mechanisms for formation of HF_4TCNQ^- in F_4TCNQ-doped rr-P3HT films with thermal annealing.

through electron rearrangement. This mechanism is essentially identical to that proposed by Northrup for degradation of P3HT,[45] with the abstracted hydrogen in this case, undergoing a radical combination with $F_4TCNQ^{\bullet-}$. The second proposed mechanism involves first a reduction of F_4TCNQ^- by the polaron $P3HT^{\bullet+}$ to form F_4TCNQ^{2-} and the bipolaron state of P3HT ($P3HT^{2+}$). The aliphatic carbon alpha to the 3-position of the bipolaron thiophene ring then engages in a rapid or coupled proton transfer to F_4TCNQ^{2-} followed by subsequent electronic rearrangement of the P3HT. Both mechanisms lead to formation of HF_4TCNQ^- and $[P3HT- H]^+$ and both are plausible given the known reaction chemistry of these and other organic materials.[44, 46-47] However, two pieces of evidence in combination suggest mechanism 1 is more likely. The first piece of evidence is the absence of a bipolaron P3HT absorption band in the UV-vis spectra at energies <1.2 eV, although admittedly, the small oscillator strength of this bipolaron band[48] renders this piece of evidence insufficient by itself. The second piece of evidence that argues against mechanism 2 is the absence of any signatures in the ν(C≡N) region of the FTIR spectra for F_4TCNQ^{2-}, which has

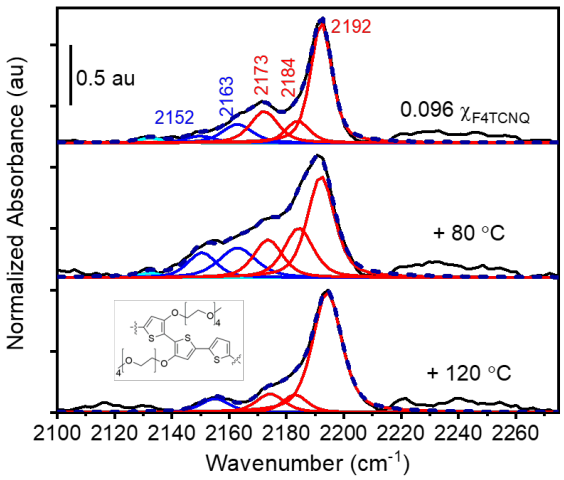

Figure 3. (a) Spectrally decomposed FTIR spectra at three temperatures during progressive heating of a 15 nm-thick film of 0.096 χ_{F4TCNQ}-doped p($g_4$2T-T). Fit peaks in red correspond to the ICT state, fit peaks in blue correspond to the dianion state. Inset depicts the p($g_4$2T-T) structure.

two relatively intense vibrational modes at distinct frequencies in this region.[38] In combination, these two pieces of evidence suggest that the mechanism 1 is more likely.

As a further test of these mechanisms, F_4TCNQ-doped films of the polymer p($g_4$2T-T)[24] were examined under identical thermal annealing conditions. Instead of hexyl side chains, this polymer possesses tetraethylene glycol side chains, and thus, does not have methylene groups at the alpha position on the 3-position of the thiophene rings (see inset structure in Figure 3). If either of the above mechanisms for HF_4TCNQ^- formation with P3HT is correct, no formation of HF_4TCNQ^- would be expected with p($g_4$2T-T). FTIR results from thermal annealing studies of F_4TCNQ-doped p($g_4$2T-T) are shown in Figure 3. We observe only a change in the ratio of the dianion state (blue peaks) co-present with the ICT state in the film (red peaks); no growth of the HF_4TNCQ^- bands at 2188 and 2154 cm^{-1} are observed. These results are in agreement with recent literature that has demonstrated greater functional stability of F_4TCNQ-doped p($g_4$2T-T) films upon heating relative to doped rr-P3HT.[24] This greater functional stability of F_4TCNQ-doped p($g_4$2T-T) is similar to that of F_4TCNQ-doped s-P3MEET, both of which are missing aliphatic methylene carbon atoms alpha to the 3-position of the thiophene rings.[25] Thus, this stabilization is the result of mitigation of the reaction chemistry as opposed to the prevention of F_4TCNQ dopant sublimation.

Through this work, we have shown conclusively that the instability of F_4TCNQ doped rr-P3HT films at temperatures between 60 and 120 °C is due to thermally-activated reaction chemistry at the aliphatic carbon atoms alpha to the 3-position of thiophene rings to form HF_4TCNQ^-, a non-chromophoric weak dopant, resulting in significant degradation of the functional properties of these films. Although exposure to light appears to have essentially no effect on this chemistry (see Figure S2), the effect of atmospheric conditions on this chemistry is being systematically explored and will be reported a later date. In total, this work codifies previously observed behaviors of different conjugated thiophene-based organic semiconducting polymers in the framework of a molecular description of relevant reaction chemistry as a rationalization for degradation of functional properties in some systems but not others. These results elucidate an important design guideline for thiophene-based active layer materials that any structural modifications of thiophene rings to enhance other properties such as solubility or processability should not contain any possibly reactive hydrogen atoms alpha to the ring 3-position.

ACKNOWLEDGEMENTS

The authors acknowledge support of this research by the National Science Foundation under award DMR-1608289. K.E.W. acknowledges financial support through an ARCS Foundation Scholarship and an ACS Division of Analytical Chemistry Fellowship sponsored by Eli Lilly and Company. M.M and I.M. acknowledge generous funding from KAUST for financial support. The authors also acknowledge very useful discussions with Professor Richard S. Glass regarding mechanistic aspects of this work. Use of the Stanford Synchrotron Radiation Lightsource, SLAC

National Accelerator Laboratory is supported by the U.S. Department of Energy, Office of Science, Office of Basic Energy Sciences under Contract No. DE-AC02-76SF00515.

SUPPLEMENTARY INFORMATION

The Supporting Information section contains unnormalized FTIR spectra of the ν(C≡N) region for three F_4TCNQ mole fraction subjected to progressive heating, pictorial representations and assignments of ν(C≡N) vibrational modes for each F_4TCNQ species, and FTIR spectra of the ν(C=C) region for 0.096 χ_{F4TCNQ} subjected to progressive heating and grazing incidence wide angle x-ray scattering data of a 0.096 χ_{F4TCNQ} subjected to progressive heating in a nitrogen glove box. The Supporting Information is available free of charge on the ACS Publications website at DOI: XXXXXXXX.

REFERENCES

1. Treat, N. D.; Shuttle, C. G.; Toney, M. F.; Hawker, C. J.; Chabinyc, M. L., In situ measurement of power conversion efficiency and molecular ordering during thermal annealing in P3HT:PCBM bulk heterojunction solar cells. *J. Mater. Chem.* **2011**, *21*, 15224-15231.
2. Glaudell, A. M.; Cochran, J. E.; Patel, S. N.; Chabinyc, M. L., Impact of the Doping Method on Conductivity and Thermopower in Semiconducting Polythiophenes. *Adv. Energy Mater.* **2015**, *5*, 1401072.
3. Zuo, G.; Andersson, O.; Abdalla, H.; Kemerink, M., High thermoelectric power factor from multilayer solution-processed organic films. *Appl. Phys. Lett.* **2018**, *112*, 083303.
4. Hynynen, J.; Kiefer, D.; Müller, C., Influence of crystallinity on the thermoelectric power factor of P3HT vapour-doped with F4TCNQ. *RSC Adv.* **2018**, *8*, 1593-1599.

5. Fukagawa, H.; Sasaki, T.; Tsuzuki, T.; Takei, T.; Motomura, G.; Hasegawa, M.; Morii, K.; Shimizu, T., Long-Lived Flexible Displays Employing Efficient and Stable Inverted Organic Light-Emitting Diodes. *Adv. Mater.* **2018**, *30*, 1706768.

6. Zhao, W.; Li, S.; Yao, H.; Zhang, Y.; Yang, B.; Hou, J., Molecular Optimization Enables over 13% Efficiency in Organic Solar Cells. *J. Am. Chem. Soc.* **2017**, *139*, 7148-7151.

7. Zhang, S.; Qin, Y.; Zhu, J.; Hou, J., Over 14% Efficiency in Polymer Solar Cells Enabled by a Chlorinated Polymer. *Adv. Mater.* **2018**, *30*, 1800868.

8. Che, X.; Li, Y.; Qu, Y.; Forrest, S. R., High Fabrication Yield Organic Tandem Photovoltaics Combining Vacuum- and Solution-Processed Subcells with 15% Efficiency. *Nature Energy* **2018**, *3*, 422.

9. Meng, L., et al., Organic and Solution-Processed Tandem Solar Cells with 17.3% Efficiency. *Science* **2018**, *361*, 1094-1098.

10. Li, G.; Zhu, R.; Yang, Y., Polymer Solar Cells. *Nat. Photonics* **2012**, *6*, 153-161.

11. Lüssem, B.; Tietze, M. L.; Kleemann, H.; Hoßbach, C.; Bartha, J. W.; Zakhidov, A.; Leo, K., Doped organic transistors operating in the inversion and depletion regime. *Nature Commun.* **2013**, *4*, 2775.

12. Bu, L.; Hu, M.; Lu, W.; Wang, Z.; Lu, G., Printing Semiconductor–Insulator Polymer Bilayers for High-Performance Coplanar Field-Effect Transistors. *Adv. Mater.* **2018**, *30*, 1704695.

13. Brixi, S.; A. Melville, O.; T. Boileau, N.; H. Lessard, B., The influence of air and temperature on the performance of PBDB-T and P3HT in organic thin film transistors. *J. Mater. Chem. C* **2018**, *6*, 11972-11979.

14. Yang, Z.; Han, S.; Liu, Y.; Zhuang, X.; Akinwande, D.; Yu, J., Investigation of the atmosphere influence on device characteristics and NO2 sensing performance of organic field-effect transistors consisting of polymer bulk heterojunction. *Org. Electronics* **2018**, *62*, 114-120.

15. Wang, Z.; Zou, Y.; Chen, W.; Huang, Y.; Yao, C.; Zhang, Q., The Role of Weak Molecular Dopants in Enhancing the Performance of Solution-Processed Organic Field-Effect Transistors. *Adv. Elec. Mater.* **2019**, *5*, 1800547.

16. Jacobs, I. E.; Moulé, A. J., Controlling Molecular Doping in Organic Semiconductors. *Adv. Mater.* **2017**, *29*, 1703063.

17. Duong, D. T.; Wang, C.; Antono, E.; Toney, M. F.; Salleo, A., The chemical and structural origin of efficient p-type doping in P3HT. *Org. Electronics* **2013**, *14*, 1330-1336.

18. Méndez, H., et al., Doping of Organic Semiconductors: Impact of Dopant Strength and Electronic Coupling. *Angew. Chem.* **2013**, *125*, 7905-7909.

19. Méndez, H., et al., Charge-transfer crystallites as molecular electrical dopants. *Nature Commun.* **2015**, *6*, 1-11.

20. Neelamraju, B.; Watts, K. E.; Pemberton, J. E.; Ratcliff, E. L., Correlation of Coexistent Charge Transfer States in F_4TCNQ-Doped P3HT with Microstructure. *J. Phys. Chem. Lett.* **2018**, *9*, 6871-6877.

21. Watts, K. E.; Neelamraju, B.; Ratcliff, E. L.; Pemberton, J. E., Stability of Charge Transfer States in F4TCNQ-Doped P3HT. *Chem. Mater.* **2019**, *31*, 6986-6994.

22. Manceau, M.; Rivaton, A.; Gardette, J.-L.; Guillerez, S.; Lemaître, N., The mechanism of photo- and thermooxidation of poly(3-hexylthiophene) (P3HT) reconsidered. *Polym. Degrad. Stab.* **2009**, *94*, 898-907.

23. Jacobs, I. E.; Cendra, C.; Harrelson, T. F.; Bedolla Valdez, Z. I.; Faller, R.; Salleo, A.; Moulé, A. J., Polymorphism controls the degree of charge transfer in a molecularly doped semiconducting polymer. *Mater. Horiz.* **2018**, 655-660.

24. Kroon, R.; Kiefer, D.; Stegerer, D.; Yu, L.; Sommer, M.; Müller, C., Polar Side Chains Enhance Processability, Electrical Conductivity, and Thermal Stability of a Molecularly p-Doped Polythiophene. *Adv. Mater.* **2017**, *29*, 1700930.

25. Li, J.; Rochester, C. W.; Jacobs, I. E.; Aasen, E. W.; Friedrich, S.; Stroeve, P.; Moulé, A. J., The effect of thermal annealing on dopant site choice in conjugated polymers. *Org. Electronics* **2016**, *33*, 23-31.

26. Li, J.; Rochester, C. W.; Jacobs, I. E.; Friedrich, S.; Stroeve, P.; Riede, M.; Moulé, A. J., Measurement of Small Molecular Dopant F4TCNQ and C60F36 Diffusion in Organic Bilayer Architectures. *ACS Appl. Mater. Interfaces* **2015**, *7*, 28420-28428.

27. Hase, H.; O'Neill, K.; Frisch, J.; Opitz, A.; Koch, N.; Salzmann, I., Unraveling the Microstructure of Molecularly Doped Poly(3-hexylthiophene) by Thermally Induced Dedoping. *J. Phys. Chem. C* **2018**, *122*, 25893-25899.

28. Untilova, V.; Biskup, T.; Biniek, L.; Vijayakumar, V.; Brinkmann, M., Control of Chain Alignment and Crystallization Helps Enhance Charge Conductivities and Thermoelectric Power Factors in Sequentially Doped P3HT:F4TCNQ Films. *Macromolecules* **2020**, *53*, 2441-2453.

29. Li, J., et al., Quantitative Measurements of the Temperature-Dependent Microscopic and Macroscopic Dynamics of a Molecular Dopant in a Conjugated Polymer. *Macromolecules* **2017**, *50*, 5476-5489.

30. Pingel, P.; Zhu, L.; Park, K. S.; Vogel, J.-O.; Janietz, S.; Kim, E.-G.; Rabe, J. P.; Brédas, J.-L.; Koch, N., Charge-Transfer Localization in Molecularly Doped Thiophene-Based Donor Polymers. *J. Phys. Chem. Lett.* **2010**, *1*, 2037-2041.

31. Meneghetti, M.; Pecile, C., Charge–transfer organic crystals: Molecular vibrations and spectroscopic effects of electron–molecular vibration coupling of the strong electron acceptor TCNQF $_4$. *J. Chem. Phys.* **1986**, *84*, 4149-4162.

32. Kampar, E.; Neilands, O., Degree of Charge Transfer in Donor–Acceptor Systems of the π–π Type. *Russ. Chem. Rev.* **1986**, *55*, 334-342.

33. Müller, L., et al., Charge-Transfer–Solvent Interaction Predefines Doping Efficiency in p-Doped P3HT Films. *Chem. Mater.* **2016**, *28*, 4432-4439.

34. Dixon, D. A.; Calabrese, J. C.; Miller, J. S., Crystal and Molecular Structure of the 2:1 Charge-Transfer Salt of Decamethylferrocene and Perfluoro-7,7,8,8-Tetracyano-p-Quinodimethane: [[Fe(C5Me5)2]+.Cntdot.]2[TCNQF4]2-. The Electronic Structure of [TCNQF4]n (n = 0, 1-, 2-). *J. Phys. Chem.* **1989**, *93*, 2284–2291.

35. Lu, J.; Le, T. H.; Traore, D. A. K.; Wilce, M.; Bond, A. M.; Martin, L. L., Synthetic Precursors for TCNQF42– Compounds: Synthesis, Characterization, and Electrochemical Studies of (Pr4N)2TCNQF4 and Li2TCNQF4. *J. Org. Chem.* **2012**, *77*, 10568-10574.

36. Le, T. H.; Nafady, A.; Qu, X.; Martin, L. L.; Bond, A. M., Detailed Electrochemical Analysis of the Redox Chemistry of Tetrafluorotetracyanoquinodimethane TCNQF4, the Radical Anion [TCNQF4]•–, and the Dianion [TCNQF4]2– in the Presence of Trifluoroacetic Acid. *Anal. Chem.* **2011**, *83*, 6731-6737.

37. Haworth, N. L.; Lu, J.; Vo, N.; Le, T. H.; Thompson, C. D.; Bond, A. M.; Martin, L. L., Diagnosis of the Redox Levels of TCNQF4 Compounds Using Vibrational Spectroscopy. *ChemPlusChem* **2014**, *79*, 962-972.

38. Watts, K. E.; Clary, K. E.; Lichtenberger, D. L.; Pemberton, J. E., FTIR Spectroelectrochemistry of F4TCNQ Reduction Products and Their Protonated Forms. *Anal. Chem.* **2020**, *92*, 7154-7161.

39. Wells, S. K.; Giergiel, J.; Land, T. A.; Lindquist, J. M.; Hemminger, J. C., Beam-induced modifications of TCNQ multilayers. *Surface Sci.* **1991**, *257*, 129-145.

40. Lindquist, J. M.; Hemminger, J. C., High-resolution core level photoelectron spectra of solid TCNQ: determination of molecular orbital spatial distribution from localized shake-up features. *J. Phys. Chem.* **1988**, *92*, 1394-1396.

41. Coletti, C.; Riedl, C.; Lee, D. S.; Krauss, B.; Patthey, L.; von Klitzing, K.; Smet, J. H.; Starke, U., Charge neutrality and band-gap tuning of epitaxial graphene on SiC by molecular doping. *Phys. Rev. B* **2010**, *81*, 235401.

42. Koch, N.; Duhm, S.; Rabe, J. P.; Vollmer, A.; Johnson, R. L., Optimized Hole Injection with Strong Electron Acceptors at Organic-Metal Interfaces. *Phys. Rev. Lett.* **2005**, *95*, 237601.

43. Manceau, M.; Gaume, J.; Rivaton, A.; Gardette, J.-L.; Monier, G.; Bideux, L., Further insights into the photodegradation of poly(3-hexylthiophene) by means of X-ray photoelectron spectroscopy. *Thin Solid Films* **2010**, *518*, 7113-7118.

44. Aoyama, Y.; Yamanari, T.; Murakami, T. N.; Nagamori, T.; Marumoto, K.; Tachikawa, H.; Mizukado, J.; Suda, H.; Yoshida, Y., Initial photooxidation mechanism leading to reactive radical formation of polythiophene derivatives. *Polym. J.* **2015**, *47*, 26-30.

45. Street, R. A.; Northrup, J. E.; Krusor, B. S., Radiation Induced Recombination Centers in Organic Solar Cells. *Phys. Rev. B* **2012**, *85*, 205211.

46. Mayer, J. M.; Hrovat, D. A.; Thomas, J. L.; Borden, W. T., Proton-Coupled Electron Transfer versus Hydrogen Atom Transfer in Benzyl/Toluene, Methoxyl/Methanol, and Phenoxyl/Phenol Self-Exchange Reactions. *J. Amer. Chem. Soc.* **2002**, *124*, 11142-11147.

47. Olivella, S.; Anglada, J. M.; Solé, A.; Bofill, J. M., Mechanism of the Hydrogen Transfer from the OH Group to Oxygen-Centered Radicals: Proton-Coupled Electron-Transfer versus Radical Hydrogen Abstraction. *Chem. Eur. J.* **2004**, *10*, 3404-3410.

48. Enengl, C.; Enengl, S.; Pluczyk, S.; Havlicek, M.; Lapkowski, M.; Neugebauer, H.; Ehrenfreund, E., Doping-Induced Absorption Bands in P3HT: Polarons and Bipolarons. *ChemPhysChem* **2016**, *17*, 3836-3844.